Balancing the Quantum Speed Limit and Instantaneous Energy Cost in Adiabatic Quantum Evolution

Jianwen Xu(徐建文)[1,2†], Yujia Zhang(张宇佳)[1,2†], Wen Zheng(郑文)[1,2†*], Haoyang Cai(蔡浩阳)[1,2], Haoyu Zhou(周浩宇)[1,2], Xianke Li(李先科)[1,2], Xudong Liao(廖绪东)[1,2], Yu Zhang(张钰)[1,2,3], Shaoxiong Li(李邵雄)[1,2,3], Dong Lan(兰栋)[1,2,3], Xinsheng Tan(谭新生)[1,2,3*], and Yang Yu(于扬)[1,2,3*]

[1]*National Laboratory of Solid State Microstructures, School of Physics, Nanjing University, Nanjing 210093, China*
[2]*Shishan Laboratory, Suzhou Campus of Nanjing University, Suzhou 215163, China*
[3]*Hefei National Laboratory, Hefei 230088, China*

(Received 28 February 2024; accepted manuscript online 26 March 2024)

Adiabatic time-optimal quantum controls are extensively used in quantum technologies to break the constraints imposed by short coherence times. However, practically it is crucial to consider the trade-off between the quantum evolution speed and instantaneous energy cost of process because of the constraints in the available control Hamiltonian. Here, we experimentally show that using a transmon qubit that, even in the presence of vanishing energy gaps, it is possible to reach a highly time-optimal adiabatic quantum driving at low energy cost in the whole evolution process. This validates the recently derived general solution of the quantum Zermelo navigation problem, paving the way for energy-efficient quantum control which is usually overlooked in conventional speed-up schemes, including the well-known counter-diabatic driving. By designing the control Hamiltonian based on the quantum speed limit bound quantified by the changing rate of phase in the interaction picture, we reveal the relationship between the quantum speed limit and instantaneous energy cost. Consequently, we demonstrate fast and high-fidelity quantum adiabatic processes by employing energy-efficient driving strengths, indicating a promising strategy for expanding the applications of time-optimal quantum controls in superconducting quantum circuits.

DOI: 10.1088/0256-307X/41/4/040202

Quantum adiabatic control plays an important role in almost all areas of quantum physics.[1–7] However, it encounters serious limitation for quantum platforms with short decoherence times, such as superconducting quantum circuits,[8,9] since it requires the sufficiently slow change of Hamiltonian in the whole quantum evolution process.[10–13] In recent years, speeding up adiabatic processes has garnered increasing attention, and various approaching paths have emerged, e.g., designing new adiabatic conditions to break the constraints of the traditional approximation adiabatic condition,[14–20] extending the classical optimal control theory to quantum systems[21,22] for exploring the time-optimal adiabatic trajectory,[23,24] and using shortcut-to-adiabaticity (STA) techniques,[25,26] such as counter-diabatic (CD) driving,[27] to suppress non-adiabatic transitions. The typical control Hamiltonian used in the above-mentioned approaches usually fail to balance the quantum speed limit (QSL) and the instantaneous energy cost.[28,29]

The QSL refers to the minimum time required for a quantum system to evolve from one state to another. Two well-known formulae are the Mandelstam–Tamm (MT)[30] and Margolus–Levitin (ML)[31] relations, which establish a lower bound on the evolution time in closed quantum systems under unitary evolution with a time-independent Hamiltonian.[32] Subsequent developments in the field have expanded these formulae to address a broader range of quantum complexities, including time-dependent Hamiltonian,[33–35] open quantum systems,[36–40] and many-body systems,[41–43] etc. The QSL can be applied to quantum systems immersed in a field that cannot be altered by the control Hamiltonian, which is also known as the quantum Zermelo navigation problem.[44–46] The energy cost of adiabatic evolutions in such systems has been studied by Garcia *et al.*[47]

In quantum platforms, particularly in light of the weak anharmonicity of transmons,[48–51] it is essential to optimize the instantaneous energy cost to meet the constraints imposed by the available Hamiltonian. At the same time, the optimizing of the cost is particularly important for large scale quantum operations, since heat-loading,[52] cross-talk,[53–56] and potential activation of two-level defects[57] by driving energy are major concerns for scaling up quantum chip.[58–63] However, based on the above-mentioned theoretical frameworks, how to balance the QSL and instantaneous energy cost remains a challenging endeavor in adiabatic time-optimal quantum controls.

In this work, in the interaction picture, we reveal the

†These authors contributed equally to this work.
*Corresponding authors. Email: zhengwen@nju.edu.cn; tanxs@nju.edu.cn; yuyang@nju.edu.cn
© 2024 Chinese Physical Society and IOP Publishing Ltd

relationship between the QSL and instantaneous energy cost in quantum adiabatic evolution according to the QSL bound, as quantified by the changing rate of phase, introduced by Sun *et al.* in 2021.[37] Then, we design the control Hamiltonian and experimentally validate the general solution of the quantum Zermelo navigation problem in a transmon. Our comprehensive study delves into the adiabatic properties and control fidelities, demonstrating the effectiveness of this approach in accelerating quantum evolution while minimizing energy costs.

Protocol Description. To describe our experimental protocol, we focus on accelerating the adiabatic quantum evolution, evolving from an initial state $|\psi_{\rm i}\rangle$ to the target state $|\psi_{\rm f}\rangle$, while at a low instantaneous energy cost throughout the evolution process. As illustrated in Fig. 1(a), when speeding up the process, the system driven by $H_0(t)$ fails to meet the adiabatic condition,[13] leading to non-adiabatic transitions and deviations from the target state. In contrast to the CD driving detailed by Berry,[27] the fundamental purpose of our protocol is quantifying the deviation of the final state $|\psi_{\rm f}'\rangle$ from the target state $|\psi_{\rm f}\rangle$. This deviation is quantified by the fidelity measure

$$\mathcal{F}_0 = |\langle\psi_{\rm i}|\psi_{\rm f}'\rangle|^2, \tag{1}$$

defined within the rotation frame of $H_0(t)$. The final state, driven by $H_0(t)$, can be written as $|\psi_{\rm f}'\rangle = \mathcal{U}_0^\dagger(\tau)|\psi_{\rm f}\rangle$, where τ is the evolution time, $\mathcal{U}_0(\tau) = \mathcal{T}\exp[-i\int_0^\tau H_0(t)dt]$ denotes the unitary rotation with the time-ordering operator $\mathcal{T}$.

To counter the deviation, we construct a control Hamiltonian $H_{\rm c}(t)$ through the following steps: First, in the presence of non-adiabatic transitions, indicated by $\mathcal{F}_0 < 1$, a state space $\bar{\mathcal{S}}$ spanned by states $|\psi_{\rm i}\rangle$ and $|\bar{\psi}_{\rm f}'\rangle$ is formed in the rotation frame of $H_0(t)$.[64] This naturally leads to the shortest evolution path, denoted as $\mathcal{L}_{\rm FS}$ also called the Fubini–Study metric, follows a geodesic trajectory, as shown in Fig. 1(b). Here, $|\bar{\psi}_{\rm f}'\rangle = (1/\sqrt{1-s^2})(|\psi_{\rm f}'\rangle - se^{i\beta}|\psi_{\rm i}\rangle)$ represents the orthonormalized final state, and $\langle\psi_{\rm i}|\psi_{\rm f}'\rangle = se^{i\beta}$ defines the corresponding parameters s and β.

Second, it is important to note that the original evolution becomes a process evolving from state $|\psi_{\rm f}'\rangle$ to state $|\psi_{\rm i}\rangle$ with an ansatz-free $H_{\rm c}'(t)$. Under the transversality condition in space $\bar{\mathcal{S}}$, the control Hamiltonian in the rotation frame is

$$H_{\rm c}'(t) = \frac{i\mathcal{C}'(t)}{\sqrt{1-s^2}}\left(e^{-i\beta}|\psi_{\rm f}'\rangle\langle\psi_{\rm i}| - e^{-i\beta}|\psi_{\rm i}\rangle\langle\psi_{\rm f}'|\right), \tag{2}$$

and hence $H_{\rm c}(t) = U_0(t)H_{\rm c}'(t)U_0^\dagger(t)$ in experiment. The instantaneous energy cost defined in this work expressed as $\mathcal{C}'(t) = \|H_{\rm c}'(t)\|$ directly relates to the energy resource required for control, as discussed in previous works.[28,29,47] This concept establishes a direct relation between the QSL and instantaneous energy cost which can be written as

$$\tau_{\rm QSL} = \frac{\mathcal{L}_{\rm FS}}{\frac{1}{\tau}\int_0^\tau \mathcal{C}'(t)dt}. \tag{3}$$

Here, the QSL is quantified by the phase changing rate,[37] also equivalent to the instantaneous energy cost, expressed as $\mathcal{C}'(t) = \partial\varphi(t)'/\partial t$ with $\varphi'(t) = \langle\psi'(t+dt)|\psi'(t)\rangle/|\langle\psi'(t+dt)|\psi'(t)\rangle|$. See the Supplementary Information (Note 1) for more details.

Lastly, in the total Hamiltonian $H(t) = H_0(t) + H_{\rm c}(t)$, as shown in Fig. 1(c), a time-optimal adiabatic trajectory at a low instantaneous energy cost can be determined, and the maximum instantaneous energy cost we concerned is denoted as

$$\mathrm{Max}[\mathcal{C}(t)] = \mathrm{Max}\|H_{\rm c}(t)\|, \tag{4}$$

where Max[ ] denotes the selection of the maximum value during the process within the time interval $t \in [0, \tau]$, and $\|H_{\rm c}(t)\| = \sqrt{\mathrm{Tr}[H_{\rm c}^2(t)]/2}$ is calculated by the Frobenius norm.

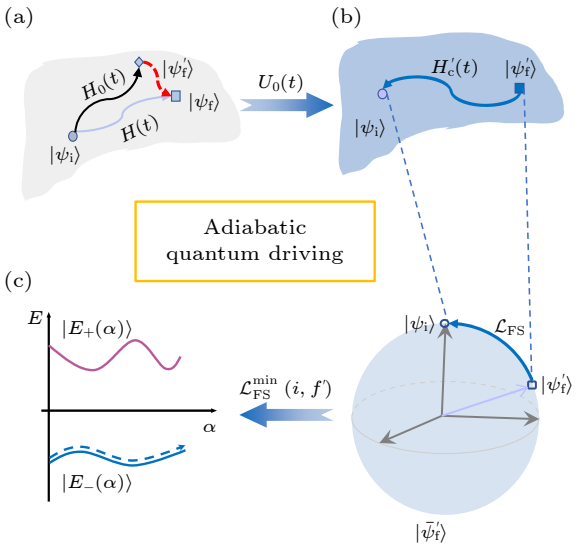

Fig. 1. Adiabatic quantum evolution. (a) The adiabatic process driven by the system Hamiltonian $H_0(t)$ can not evolve the initial state $|\psi_{\rm i}\rangle$ to the target state $|\psi_{\rm f}\rangle$ due to the non-adiabatic transition. By introducing a suitable control Hamiltonian $H_{\rm c}(t)$, the adiabatic process can be realized within the total Hamiltonian $H(t)$. (b) Within the rotation frame of $H_0(t)$, the process becomes from $|\psi_{\rm f}'\rangle$ evolving $|\psi_{\rm i}\rangle$ under the control Hamiltonian $H_{\rm c}'(t)$. The minimum evolution path is the state evolving along the geodesic in a space spanned by states $|\psi_{\rm i}\rangle$ and $|\psi_{\rm f}'\rangle$. (c) The control Hamiltonian can be acquired according to Eq. (2). The optimal adiabatic trajectory is identified with balancing the QSL and instantaneous energy cost.

Experimental Results. In experiment, the transmon we used possesses an anharmonicity of $\alpha/2\pi = -268\,\mathrm{MHz}$, and the transition frequency between the lowest two energy levels of $\omega_q/2\pi = 5\,\mathrm{GHz}$. The measured energy relaxation time is $T_1 = 22.5\,\mu\mathrm{s}$, and the dephasing time, determined by Ramsey fringes experiment, is $T_2^\star = 12.3\,\mu\mathrm{s}$. See the Supplementary Information (Note 2) for more details about our experimental setup. In the presence of a microwave driving field, the system Hamiltonian is given by $H(t) = \omega_q a^\dagger a + \frac{\alpha}{2}a^\dagger a^\dagger aa + \Omega(t)\cos[\omega_d(t)t + \phi(t)](a^\dagger + a)$, where a ($a^\dagger$) represents the annihilation (creation) operator. The terms $\omega\psi_{\rm d}(t)$, $\Omega(t)$, and $\phi(t)$ denote the driving

frequency, strength, and phase, respectively. These parameters are finely tuned on base of interference experiments.

In the regime where the transmon driving strength is much weaker than its anharmonicity, the system can be effectively described using rotation wave approximation. This simplifies the system dynamics, leading to the Landau–Zener (LZ) Hamiltonian, a cornerstone in quantum physics.[65,66] We express the Hamiltonian as $H_0(t) = \frac{\Omega_0}{2}\sigma_x + \frac{\Delta(t)}{2}\sigma_z$. Its instantaneous eigenstates $|E_-(t)\rangle = \sin\frac{\theta(t)}{2}|0\rangle - \cos\frac{\theta(t)}{2}|1\rangle$ and $|E_+(t)\rangle = \cos\frac{\theta(t)}{2}|0\rangle + \sin\frac{\theta(t)}{2}|1\rangle$, with corresponding eigenenergies $E_\pm(t) = \pm\frac{1}{2}\sqrt{\Delta^2(t)+\Omega_0^2}$, are derived, where $\Delta(t)$ represents the detuning, Ω_0 is the coupling between the diabatic levels, with $\theta(t) = \arctan\frac{\Omega_0}{\Delta(t)}$.

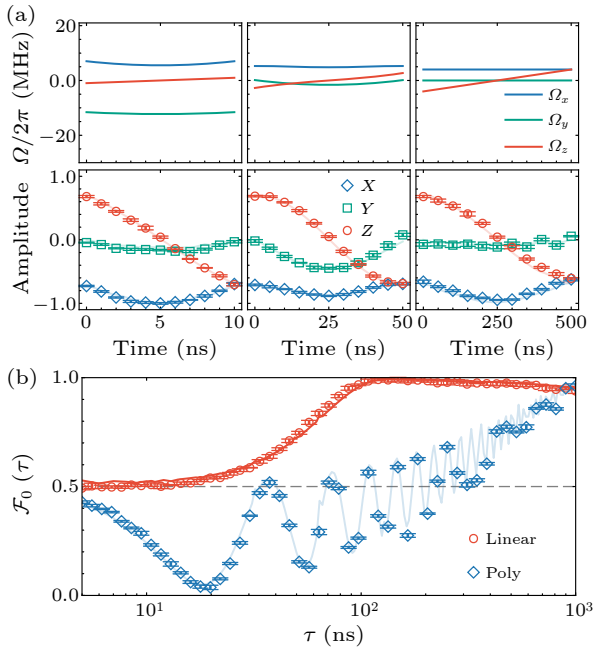

Fig. 2. Adiabatic quantum drivings versus evolution time τ. (a) The driving pulses (upper panel) in the left-to-right subplots are calculated with $\tau = 10$ ns, 50 ns, and 500 ns, respectively. The lower panel shows the corresponding state trajectories acquired by quantum state tomography. The coupling strength is set to $\Omega_0/2\pi = 8$ MHz. (b) The fidelity $\mathcal{F}_0$ dictated solely by the drift Hamiltonian H_0 against evolution time τ. The experiment results (points) are in agreement with the simulation one (lines), while the red (blue) symbols indicate the linear (polynomial) detuning function.

First, we use LZ Hamiltonian to demonstrate how to balance the QSL and energetic cost in quantum adiabatic controls. We design an adiabatic trajectory from the initial state $|\psi_\mathrm{i}\rangle$ corresponding to $|E_-\rangle$ at $\theta = 3\pi/4$, to the target state $|\psi_\mathrm{f}\rangle$ equivalent to $|E_-\rangle$ at $\theta = \pi/4$. The driving pulses $\boldsymbol{\Omega}_\mathrm{c}(t) = \mathrm{Tr}[H_\mathrm{c}(t)\boldsymbol{\sigma}]/2$ are required according to Eq. (2), where $\boldsymbol{\sigma} = \sigma_x, \sigma_y, \sigma_z$ are the Pauli matrices. Using Eq. (3), the optimal instantaneous energy cost is determined under three distinct speed limits: 10 ns, 50 ns, and 500 ns, with parameters including $\Omega_0/2\pi = 8$ MHz, $\Delta_0/2\pi = 8$ MHz, and the linear detuning function $\Delta_\mathrm{linear}(t) = 2\Delta_0(t/\tau - 1/2)$. Unless otherwise specified, we set $\mathcal{C}'(t)$ to be a constant denoted as ν_z. The driving pulses calculated in routine are illustrated in the upper panel of Fig. 2(a). When applied to our transmon, these pulses yield three evolution trajectories, represented as symbols in the lower panel of Fig. 2(a). These trajectories are in good agreement with our simulation results, plotted as lines. In this work, the error bars represent standard deviation. At the end of the evolution, the fidelities of the target state are 0.996 ± 0.007, 0.988 ± 0.004, and 0.935 ± 0.008, while in simulation, they are 1.000, 0.997, and 0.981, respectively. The formula of the state fidelity is defined as

$$\mathcal{F} = \mathrm{Tr}(\sqrt{\rho_\mathrm{ideal}}\rho_\mathrm{exp}\sqrt{\rho_\mathrm{ideal}}), \tag{5}$$

with the ideal target state $\rho_\mathrm{ideal} = |\psi_\mathrm{f}\rangle\langle\psi_\mathrm{f}|$ and the final state ρ_exp.

In Fig. 2(b), we investigate the adiabaticity by the fidelity $\mathcal{F}_0$, under various adiabatic processes dictated by the Hamiltonian $H_0(t)$. Our speed choices yield span a broad range of adiabatic efficiencies, ranging from less favorable adiabatic processes ($\mathcal{F}_0$ near 0.5) to highly efficient ones ($\mathcal{F}_0$ approaching 1). Experimental (simulation) results under the above three speed limits reveal $\mathcal{F}_0$ values of 0.509 ± 0.008 (0.525), 0.747 ± 0.007 (0.722), and 0.975 ± 0.010 (0.975), respectively. Further analysis with a linear detuning function $\Delta_\mathrm{linear}(t)$ reveals a clear trend: the evolution speed inversely affects non-adiabatic transitions, suggesting faster processes yield smaller $\mathcal{F}_0$. Conversely, $\mathcal{F}_0$ oscillates with the evolution speed and may even approach zero, as depicted by the blue points in Fig. 2(b) by employing a polynomial detuning function expressed as $\Delta_\mathrm{poly}(t) = \frac{\Delta_0}{2}(a(t/\tau)^2 + b(t/\tau) + c)$, with initial and final conditions $\Delta_\mathrm{poly}(t = 0) = -\Delta_0$ and $\Delta_\mathrm{poly}(t = \tau) = \Delta_0$. For straightforward comparison, $a = b^2/32$ is selected, yielding specific values for $b = -16 - \sqrt{1536}/2$ and $c = -2$.

To study the impact of these two detuning functions on the evolution processes, we analyze the fidelity of the target state as a function of evolution time τ and the cost ν_z, spanning two orders of magnitude, ranging from 10 ns to 1000 ns and from 1 MHz to 100 MHz, respectively. The results of both experiment and simulation with linear and polynomial detuning functions are shown in Fig. 3. Notably, the results with high-fidelity $\mathcal{F} = 0.98$ are extracted and depicted by blue and red lines, providing clear insights into the efficiency of the evolution processes under different conditions. We reference the MT bound as a fundamental comparison, where in the absence of H_0, Eq. (3) aligns with the QSL bound, defined as $\tau_\mathrm{MT} = \frac{1}{\nu_z}\arccos|\langle\psi_\mathrm{i}|\psi_\mathrm{f}\rangle|$. This comparison, illustrated with a black dashed line in our figures, reveals that for higher ν_z, the evolution time τ approaches τ_MT, indicating a diminished influence of on the Hamiltonian $H_0(t)$. At lower ν_z, the relationship between τ and τ_MT primarily depends on the modulation of detuning $\Delta(t)$, highlighting the critical role of detuning functions in the adiabatic process efficiency.

Given ν_z, with the linear function of detuning, the evolution consistently remains below the MT bound, signifying an acceleration of the process facilitated by the Hamiltonian $H_0(t)$ and this can be directly reflected in the relation $\mathcal{F} < \mathcal{F}_0$. In the case of polynomial detuning, the evolution often surpasses the MT bound, indicating a hindrance in the process, driven by $H_0(t)$, as reflected in the relation $\mathcal{F} > \mathcal{F}_0$. Interestingly, even under the same ν_z, the polynomial detuning can shift into the acceleration regime, depending on the specific value of τ. These findings illustrate that the efficiency of adiabatic evolution in a quantum system, governed by the Hamiltonian $H_0(t)$, hinges critically on the interplay between the evolution speed and cost.

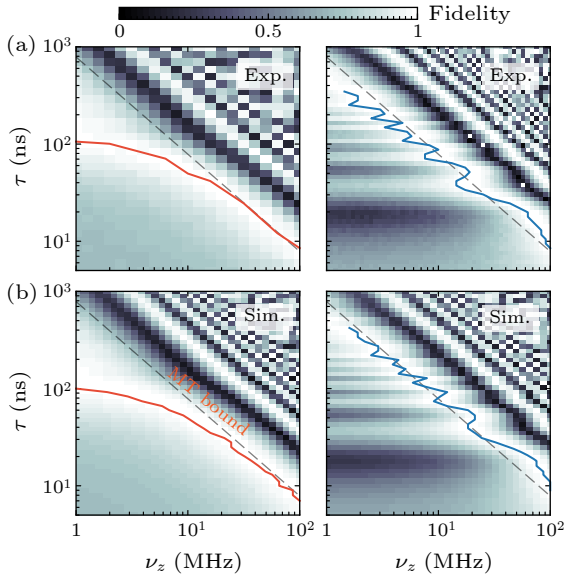

Fig. 3. Relationship between the quantum speed limit and instantaneous energy cost. (a) The fidelity of the target state versus the evolution time τ and the energy cost ν_z. The left panel is the results under the linear function of detuning $\Delta_{\text{linear}}(t)$, while the right panel is the one under the polynomial function $\Delta_{\text{poly}}(t)$. The corresponding simulation results are shown in (b). The red and blue lines represent the evolution achieving the fidelity of $F_0 = 0.98$ in the shortest time. Under $\Delta_{\text{linear}}(t)$, the red line is always below in the well-known MT bound (gray dashed lines), falling into the acceleration regime. The blue line can cross the MT bound, which steps into the acceleration or hindrance regime depending on the speed τ and cost ν_z. As the cost ν_z decreases, the boundary line closing to the MT bound.

Next, we introduce the average adiabaticity across the evolution process quantified by

$$\bar{\mathcal{A}} = \frac{1}{\tau}\int_0^\tau \mathcal{A}(t)dt, \tag{6}$$

where adiabaticity at any time t is defined as $\mathcal{A}(t) = |\langle E_-(t)|\psi(t)\rangle|^2$. Under the linear detuning, as shown in Fig. 4(a), it is revealed that even with zero coupling $\Omega_0/2\pi = 0$ MHz, the process exhibits high adiabaticity, with $\mathcal{A}(t)$ averaging around 0.82. This suggests that highly adiabatic processes are attainable even in the presence of vanishing energy gaps. Furthermore, as the coupling strength increases to $\Omega_0/2\pi = 0.2$ MHz and 10 MHz, $\bar{\mathcal{A}}$ approaches values near 0.87 and 0.98, respectively, indicating an enhancement in adiabatic fidelity.

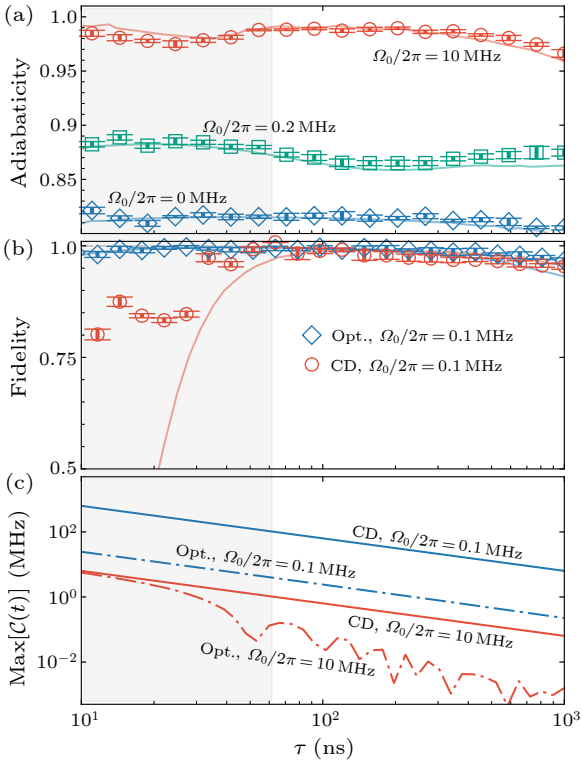

Fig. 4. (a) The average adiabaticity $\bar{\mathcal{A}}$ versus the evolution time τ. The blue, green, and red points (lines) are the experimental (simulation) results obtained according to Eq. (6). The corresponding couplings $\Omega_0/2\pi$ are set to 0, 0.2, and 10 MHz, respectively. (b) The target state fidelity against with τ. At $\Omega_0/2\pi = 0.1$ MHz, the protocol in this work (blue diamonds, labeled as Opt.) has better performance than the CD driving (red circles). When the coupling increases to 10 MHz, this protocol and CD driving have similar performance. The corresponding maximum driving strengths are shown in (c).

Finally, compared with the CD driving, this protocol exhibits a significant advantage in terms of the instantaneous energy cost throughout the evolution process. This advantage is clearly shown in Figs. 4(b) and 4(c), where our approach yields high fidelity under fast speed but low instantaneous energy cost in achieving the target state. Specifically, the notation such as CD, $\Omega_0/2\pi = 0.1$ MHz denotes the maximum instantaneous cost Max$[\mathcal{C}(t)]$ calculated under a coupling strength of 0.1 MHz using the CD driving technique, while the Opt. means the cost obtained using the protocol with balancing the QSL and cost. The limitation of CD driving stems from the control Hamiltonian, $H_{\text{cd}}(t) = \Omega_{\text{cd}}(t)\sigma_y$, which requires energy resources beyond what our experimental platform can provide. Specifically, the CD driving term, formulated as $\Omega_{\text{cd}}(t) = -\dot{\Delta}_{\text{linear}}(t)\Omega_0/2[\Omega_0^2 + \Delta_{\text{linear}}^2(t)]$ accord-

ing to Eq. (2.9) in Ref. [27], becomes unmanageable as Ω_0 approaches zero, thus presenting a challenge for practical applications. For instance, in our transmon qubit, the limitations of energy resource include that the restrictions of experimental setups make it impossible to achieve too large driving strengths. Here, we clarify that typically, Max$[\mathcal{C}(t)]$ should be less than the anharmonicity of the system. Based on our findings, particularly as observed in Figs. 4(b) and 4(c), we conclude that for the CD protocol implemented in this work, Max$[\mathcal{C}(t)]$ ideally should not exceed 100 MHz, taking into account the anharmonicity at 268 MHz. On the other hand, the too strong driving will break the approximation of the transmon two-level system due to its weak anharmonicity. Such constraints would lead to undesirable excitation of higher energy levels, thereby compromising the target state. These limitations make the failure of the CD driving, but the protocol we used still works well, offering a promising approach to achieving adiabatic time-optimal quantum controls.

To conclude, our work demonstrates the adiabatic time-optimal quantum control with minimized instantaneous energy cost in a transmon. The protocol we used differs from the CD driving by incorporating the QSL within the interaction picture, revealing a novel time-optimal protocol for adiabatic controls. This advancement not only provides a more efficient framework for adiabatic process optimization via strategic Hamiltonian manipulation but also enhances our understanding of quantum system dynamics under energy-efficient conditions. Moreover, the instantaneous energy cost is a very interesting topic concerned widely in various fields, although in quantum technologies. Our findings suggest new avenues for balancing the QSL and instantaneous energy cost in the adiabatic evolution of superconducting quantum circuits.

Acknowledgements. This work was supported by the National Natural Science Foundation of China (Grant Nos. U21A20436 and 12074179), the Innovation Program for Quantum Science and Technology (Grant No. 2021ZD0301702), the Natural Science Foundation of Jiangsu Province (Grant Nos. BE2021015-1 and BK20232002), the Jiangsu Funding Program for Excellent Postdoctoral Talent (Grant Nos. 20220ZB16 and 2023ZB562), and the Natural Science Foundation of Shandong Province (Grant No. ZR2023LZH002).

References

[1] Albash T and Lidar D A 2018 *Rev. Mod. Phys.* **90** 015002
[2] Brooke J, Bitko D, Rosenbaum F T, and Aeppli G 1999 *Science* **284** 779
[3] Farhi E, Goldstone J, Gutmann S, Lapan J, Lundgren A, and Preda D 2001 *Science* **292** 472
[4] Degen C L, Reinhard F, and Cappellaro P 2017 *Rev. Mod. Phys.* **89** 035002
[5] Georgescu I M, Ashhab S, and Nori F 2014 *Rev. Mod. Phys.* **86** 153
[6] Shi A, Guan H, Zhang J, and Zhang W 2020 *Chin. Phys. Lett.* **37** 120301
[7] Altman E, Brown K R, Carleo G *et al.* 2021 *PRX Quantum* **2** 017003
[8] Devoret M H and Schoelkopf R J 2013 *Science* **339** 1169
[9] You J Q and Nori F 2011 *Nature* **474** 589
[10] Ehrenfest P 1916 *Ann. Phys. (Berlin)* **356** 327
[11] Born M and Fock V 1928 *Z. Phys.* **51** 165
[12] Schwinger J 1937 *Phys. Rev.* **51** 648
[13] Kato T 1950 *J. Phys. Soc. Jpn.* **5** 435
[14] Wei Z H and Ying M S 2007 *Phys. Rev. A* **76** 024304
[15] Comparat D 2009 *Phys. Rev. A* **80** 012106
[16] Tong D M, Singh K, Kwek L C, and Oh C H 2007 *Phys. Rev. Lett.* **98** 150402
[17] Wang Z Y and Plenio M B 2016 *Phys. Rev. A* **93** 052107
[18] Xu K B, Xie T Y, Shi F Z, Wang Z-Y, Xu X K, Wang P F, Wang Y, Plenio M B, and Du J F 2019 *Sci. Adv.* **5** eaax3800
[19] Zheng W, Xu J W, Wang Z M, Dong Y Q, Lan D, Tan X S, and Yu Y 2022 *Phys. Rev. Appl.* **18** 044014
[20] Dodin A and Brumer P 2021 *PRX Quantum* **2** 030302
[21] Pontryagin L 1987 *Mathematical Theory of Optimal Processes* 1st edn (New York: CRC Press)
[22] Boscain U, Sigalotti M, and Sugny D 2021 *PRX Quantum* **2** 030203
[23] Martinis J M and Geller M R 2014 *Phys. Rev. A* **90** 022307
[24] Zheng W, Zhang Y, Dong Y Q *et al.* 2022 *npj Quantum Inform.* **8** 9
[25] Torrontegui E, Ibáñez S, Martínez-Garaot S, Modugno M, del Campo A, Guéry-Odelin D, Ruschhaupt A, Chen X, and Muga J G 2013 Shortcuts to adiabaticity, in *Adv. At. Mol. Opt. Phys.* vol 62 p 117, edited by Arimondo E, Berman P R, and Lin C C (Academic Press)
[26] Guéry-Odelin D, Ruschhaupt A, Kiely A, Torrontegui E, Martínez-Garaot S, and Muga J G 2019 *Rev. Mod. Phys.* **91** 045001
[27] Berry M V 2009 *J. Phys. A* **42** 365303
[28] Zheng Y J, Campbell S, De Chiara G, and Poletti D 2016 *Phys. Rev. A* **94** 042132
[29] Campbell S and Deffner S 2017 *Phys. Rev. Lett.* **118** 100601
[30] Mandelstam L and Tamm I 1991 The uncertainty relation between energy and time in non-relativistic quantum mechanics, in *Selected Papers*, edited by Bolotovskii B M, Frenkel V Y, and Peierls R (Berlin: Springer) p 115
[31] Margolus N and Levitin L B 1998 *Physica D* **120** 188
[32] Levitin L B and Toffoli T 2009 *Phys. Rev. Lett.* **103** 160502
[33] Marvian I and Lidar D A 2015 *Phys. Rev. Lett.* **115** 210402
[34] Sun S N and Zheng Y J 2019 *Phys. Rev. Lett.* **123** 180403
[35] Ness G, Alberti A, and Sagi Y 2022 *Phys. Rev. Lett.* **129** 140403
[36] Pires D P, Cianciaruso M, Céleri L C, Adesso G, and Soares-Pinto D O 2016 *Phys. Rev. X* **6** 021031
[37] Sun S N, Peng Y G, Hu X H, and Zheng Y J 2021 *Phys. Rev. Lett.* **127** 100404
[38] Wu W and An J-H 2022 *Phys. Rev. A* **106** 062438
[39] García-Pintos L P, Nicholson S B, Green J R, del Campo A, and Gorshkov A V 2022 *Phys. Rev. X* **12** 011038
[40] Dou F Q, Han M P, and Shu C C 2023 *Phys. Rev. Appl.* **20** 014031
[41] Bukov M, Sels D, and Polkovnikov A 2019 *Phys. Rev. X* **9** 011034
[42] Suzuki K and Takahashi K 2020 *Phys. Rev. Res.* **2** 032016
[43] Xu T-N, Li J, Busch T, Chen X, and Fogarty T 2020 *Phys. Rev. Res.* **2** 023125
[44] Russell B and Stepney S 2014 *Phys. Rev. A* **90** 012303
[45] Brody D C and Meier D M 2015 *Phys. Rev. Lett.* **114** 100502
[46] Bofill J M, Sanz A S, Albareda G, Moreira I d P R, and Quapp W 2020 *Phys. Rev. Res.* **2** 033492
[47] Garcia L, Bofill J M, Moreira I d P R, and Albareda G 2022 *Phys. Rev. Lett.* **129** 180402; erratum in: 2023 *Phys. Rev. Lett.* **130** 089901
[48] Koch J, Yu T M, Gambetta J, Houck A A, Schuster D I, Majer J, Blais A, Devoret M H, Girvin S M, and Schoelkopf R J 2007 *Phys. Rev. A* **76** 042319

[49] Barends R, Kelly J, Megrant A *et al.* 2013 *Phys. Rev. Lett.* **111** 080502
[50] Zhao P, Xu P, Lan D, Chu J, Tan X S, Yu H F, and Yu Y 2020 *Phys. Rev. Lett.* **125** 200503
[51] Ye Y S, Cao S R, Wu Y L, Chen X W, Zhu Q L, Li S W, Chen F S, Gong M, Zha C, Huang H L, Zhao Y, Wang S, Guo S, Qian H, Liang F, Lin J, Xu Y, Guo C, Sun L, Li N, Deng H, Zhu X, and Pan J W 2021 *Chin. Phys. Lett.* **38** 100301
[52] Krinner S, Storz S, Kurpiers P, Magnard P, Heinsoo J, Keller R, Lütolf J, Eichler C, and Wallraff A 2019 *EPJ Quantum Technol.* **6** 2
[53] Wenner J, Neeley M, Bialczak R C, Lenander M, Lucero E, O'Connell A D, Sank D, Wang H, Weides M, Cleland A N, and Martinis J M 2011 *Supercond. Sci. Technol.* **24** 065001
[54] Nuerbolati W, Han Z, Chu J, Zhou Y, Tan X, Yu Y, Liu S, and Yan F 2022 *Appl. Phys. Lett.* **120** 174001
[55] Wang R X, Zhao P, Jin Y R, and Yu H F 2022 *Appl. Phys. Lett.* **121** 152602
[56] Zhao P 2023 *Phys. Rev. Appl.* **20** 054033
[57] Müller C, Cole J H, and Lisenfeld J 2019 *Rep. Prog. Phys.* **82** 124501
[58] Sarovar M, Proctor T, Rudinger K, Young K, Nielsen E, and Blume-Kohout R 2020 *Quantum* **4** 321
[59] Zhao P, Linghu K, Li Z Y, Xu P, Wang R X, Xue G M, Jin Y R, and Yu H F 2022 *PRX Quantum* **3** 020301
[60] Zheng W, Xu J W, Ma Z, Li Y, Dong Y Q, Zhang Y, Wang X H, Sun G Z, Wu P H, Zhao J, Li S X, Lan D, Tan X, and Yu Y 2022 *Chin. Phys. Lett.* **39** 100202
[61] Zhao P, Wang R X, Hu M J, Ma T, Xu P, Jin Y, and Yu H F 2023 *Phys. Rev. Appl.* **19** 054050
[62] Zhou Z Y, Sitler R, Oda Y, Schultz K, and Quiroz G 2023 *Phys. Rev. Lett.* **131** 210802
[63] Xu S B, Sun Z Z, Wang K, Xiang L, Bao Z H, Zhu Z, Shen F, Song Z, Zhang P, Ren W, Zhang X, Dong H, Deng J, Chen J, Wu Y, Tan Z, Gao Y, Jin F, Zhu X, Zhang C, Wang N, Zou Y, Zhong J, Zhang A, Li W, Jiang W, Yu L W, Yao Y, Wang Z, Li H, Guo Q, Song C, Wang H, and Deng D L 2023 *Chin. Phys. Lett.* **40** 060301
[64] Anandan J and Aharonov Y 1990 *Phys. Rev. Lett.* **65** 1697
[65] Landau L D 1932 *Phys. Z. Sowjetunion* **2** 46
[66] Zener C 1932 *Proc. R. Soc. Lond. A* **137** 696